FEATURE DETECTION IN POLINSAR IMAGES BY AN INTERACTIVE FUZZY FUSION APPROACH. APPLICATION TO GLACIER MONITORING

G. Vasile[(1),(2),(4)], E. Trouvé[(1),(2)], L. Valet[(1)], J-M. Nicolas[(3)], M. Gay[(2)], L. Bombrun[(2)], and Ph. Bolon[(1)]

[(1)]*LISTIC, Polytech'Savoie, Annecy, FRANCE - Email: {g.vasile|trouve|valet|bolon}@univ-savoie.fr*
[(2)]*GIPSA-lab, CNRS, Grenoble, FRANCE - Email: {michel.gay|lionel.bombrun}@lis.inpg.fr*
[(3)]*GET Télécom, CNRS, Paris, FRANCE - Email: nicolas@tsi.enst.fr*
[(4)]*LAPI, University "POLITEHNICA" Bucharest, ROMANIA - Email: gvasile@alpha.imag.pub.ro*

ABSTRACT

Interferometry in POLSAR performs two acquisitions (spatially separated by the baseline) of the scattering matrix for each resolution cell. The advantages of interferometry (height and/or displacement information) are enhanced by the polarimetric decomposition techniques. In this paper a two-step approach is proposed to obtain specific features from multivariate SAR data sets, either multi-temporal InSAR or POL-InSAR. The first step consists in extracting image attributes related to the useful information. The second step consists in merging the attributes using a interactive fuzzy fusion technique. The interactive fuzzy fusion is proposed to provide end-users with a simple and easily understandable tool for tuning the detection results. A first application of the method is performed on a data set of five co-registered ERS 1/2 tandems from the French Alps (the Mont-Blanc region), including two temperate glaciers: the Argentière and the Mer-de-glace. A second application is the analysis of the scattering mechanisms with L-Band E–SAR POL-InSAR data.

Key words: POL-InSAR; fuzzy fusion; Alpine glaciers.

1. INTRODUCTION

Up to now, only 1% of the existing world temperate glaciers have been monitored [1], mostly by ground measurements which often provide information only once or twice a year at a few points. Because of the difficulty of reaching high altitude glaciers in risky mountainous areas, acquisition and processing of remotely sensed data should provide more information to improve glacier monitoring. In the Alps, in high mountain areas where the glacier activity has to be monitored, large series of spaceborne SAR (Synthetic Aperture Radar) images are often available through local environmental agencies and space agencies. But gathering multi-source data sets for a given area and extracting the desired geophysical information remain difficult tasks.

In the field of SAR interferometry (InSAR), different approaches have been applied for studying glaciers. The repeat-pass SAR acquisitions of the ERS 1/2 tandem mission has provided a large database for glacier monitoring. One of the approaches used to study small movements over large areas is differential interferometry which consists in differencing either two SAR interferograms or one interferogram and a topographical interferogram simulated by using a DTM over the same target area [2]. SAR interferometry has the potential to measure temperate glacier displacement with a large coverage compared to sparse terrestrial ground measurements [3]. Depending on the surface coverage (rocks, snow or ice), the scattering properties may change with time and induce the decrease of interferogram coherence i.e. temporal decorrelation. More recent techniques have been proposed to select in an interferogram the pixels which exhibit less decorrelation than others in order to reduce such effects within conventional InSAR processing. Several discriminant parameters were proposed for describing these coherent or stable scatterers: either within one SAR acquisition (internal coherence [4], mutual information) or in a large number of interferograms [5].

Polarimetric synthetic aperture radar (POLSAR) is an extension of the SAR imaging system, the sensors being able to emit and receive two polarizations. Monostatic polarimetric acquisitions are characterized by the 3×3 polarimetric coherency matrix. The POLSAR information allows the discrimination of different scattering mechanisms. Interferometry in POLSAR performs two acquisitions (spatially separated by the baseline) of the scattering matrix for each resolution cell. The advantages of interferometry (height and/or displacement information) are enhanced by the polarimetric decomposition techniques.

In this paper a two-step approach is proposed to obtain simultaneously spatial and temporal information from multivariate SAR data sets, either multi-temporal or POL-InSAR. The first step consists in extracting image attributes related to the useful information. The second step consists in merging the attributes using a interactive fuzzy fusion technique. The interactive fuzzy fusion is proposed to provide end-users with a simple and easily

understandable tool for tuning the detection results. The interactive aspect allows the integration of prior information, expert knowledge, and/or new available data. The symbolic aspect is about the type of effective fusion of the data: in opposition of the numerical way where the values are directly merged by numerical operators, in a symbolic way a semantic description of the data is made and the fusion is realized at the symbol level which is close to the end user reasoning.

A first application of the method is performed on a data set of five corregistered ERS 1/2 InSAR tandems from the French Alps (the Mont-Blanc region), including two temperate glaciers: the Argentière and the Mer-de-glace. The estimated attributes are: InSAR vector coherence map, the second kind cumulants (log-cumulants) and morphological attributes issued from the IDAN estimation technique [6]. The fuzzy fusion of such attributes provides information on the preservation of the coherence over the studied glaciers for velocity measurements, both on pointwise and distributed targets. Moreover, possible candidates for coherent and stable scatterers (CSS) are obtained for further CSS processing [5].

In preparation for future POLSAR/POL-InSAR data sets acquired over Alpine glaciers, this application is illustrated with L-band E-SAR data over the Oberpfaffenhofen test site. The proposed attributes are: standard H/α POLSAR parameters [7] and A_1/A_2 indices [6]. The fuzzy fusion system provide useful information on the separation of different scattering mechanisms. Such information may be used as initialization for the standard POL-InSAR Wishart clustering.

2. ATTRIBUTE ESTIMATION

The first step of the proposed approach consists in developing attributes which reveal the presence of specific features in the interferometric or polarimetric SAR images.

2.1. Multi-InSAR attributes

In Multi-InSAR processing, it is important to have a good description of both scattering properties and temporal evolution of the target area, over the whole data set.

One parameter for characterizing the stable scatterers within multiple interferograms is proposed, namely the "vector coherence" C_v. This parameter is estimated using intensity-driven Adaptive-Neighborhood AN [6] technique:

$$C_v = \frac{\sum_{k=1}^{N} \sum_{i \in AN} z_{i_k}^M z_{i_k}^{S^*}}{\sqrt{\sum_{k=1}^{N} \sum_{i \in AN} |z_{i_k}^M|^2 \cdot \sum_{k=1}^{N} \sum_{i \in AN} |z_{i_k}^S|^2}}, \quad (1)$$

where N is the number of available InSAR couples, z^M and z^S are the master and slave SLC images, respectively. In Eq. (1), it is important to notice that the local deterministic component of the phase signal ϕ should be flattened when estimating the complex correlation within the 3D adaptive neighborhood. In this paper the adaptive HR-LR model of local frequencies (f_x, f_y) [8] is used for the phase flattening:

$$\phi_{fl}(k,l) = \phi(k,l) - 2\pi[(k-m)f_x + (l-n)f_y] - \phi(m,n), \quad (2)$$

where (m,n) is the position of the central pixel within the interferogram and $(k,l) \in AN$ belong to the estimation sliding window.

A different way to detect non-homogeneous areas in multi-temporal data consists in estimating texture parameters in spatio-temporal windows made of the pixel values at the different dates in a small spatial neighborhood. For intensity images, in homogeneous areas the probability density functions (pdf) of fully developed speckle is known to be a Gamma distribution:

$$\mathcal{G}[\mu, L](x) = \frac{1}{\Gamma(L)} \frac{L}{\mu} \left(\frac{Lx}{\mu} \right)^{L-1} exp^{-\frac{Lx}{\mu}} \quad (3)$$

where L is the equivalent number of looks and μ the mean value of the intensity. Defined on $\mathbf{R}^+$, such a pdf is easily modeled by second kind characteristic functions and second kind cumulants [9]. These "log-cumulants" make the estimation of the pdf parameters simpler and more robust. With a Gamma distribution, the second and third order log-cumulants are independent of μ and directly linked to L by:

$$\tilde{\kappa}_2 = \tilde{m}_2 - \tilde{m}_1^2 = \mathbf{\Psi}'(L) \quad (4)$$

$$\tilde{\kappa}_3 = \tilde{m}_3 - 3\tilde{m}_1\tilde{m}_2 + 2\tilde{m}_1^2 = \mathbf{\Psi}''(L) \quad (5)$$

where $\tilde{m}_k$ is the k^{th} raw log-moment and $\mathbf{\Psi}'(L), \mathbf{\Psi}''(L)$ are the first and the second derivatives of the Digamma function. Estimating $\tilde{\kappa}_2$ and $\tilde{\kappa}_3$ in spatio-temporal windows provides two texture parameters which are useful to reveal spatial features and temporal changes. In homogeneous areas, $\tilde{\kappa}_2$ and $\tilde{\kappa}_3$ are close to the theoretical values $\mathbf{\Psi}'(L)$ and $\mathbf{\Psi}''(L)$ respectively. In the presence of temporal changes or spatial features, $\tilde{\kappa}_2$ values increase whereas $\tilde{\kappa}_3$ may increase or decrease depending on whether the heterogeneity creates heavy tail or heavy head distributions respectively.

Finally, a morphological attribute is obtained. When applying the IDAN region growing technique [6], the size of the adaptive neighborhood used in the estimation process is stored for each pixel. Such an attribute is well suited for detection of isolated brilliant points corresponding to strong reflectors where the window size is very small. On the contrary, distributed targets correspond to a larger window size with a homogenous cover.

2.2. POL-InSAR attributes

The POL–InSAR data is obtained by two parallel passes separated by a baseline for interferometry. By using the

Pauli basis matrices [10], the obtained coherent scattering vectors $[k]_i$ are closer to the physical phenomena of wave scattering:

$$[k]_i = \frac{1}{\sqrt{2}} \begin{bmatrix} S_{HH_i} + S_{VV_i} \\ S_{HH_i} - S_{VV_i} \\ 2S_{XX_i} \end{bmatrix}. \quad (6)$$

One complete representation of the data is the 6×6 Hermitian positive semidefinite coherency matrix:

$$[T]_6 = \begin{bmatrix} [T]_{11} & [\Omega]_{12} \\ [\Omega]^{*t}_{12} & [T]_{22} \end{bmatrix}, \quad (7)$$

where $[T]_{ii}$, $i \in \{1, 2\}$ are the 3×3 polarimetric coherency positive semidefinite Hermitian matrices from each pass, $[\Omega]_{12}$ being the interferometric coherency matrix between the polarized acquisitions:

$$[T]_{ii} = E\{[k]_i [k]^{*t}_i\} \quad \text{and} \quad [\Omega]_{12} = E\{[k]_1 [k]^{*t}_2\}. \quad (8)$$

where $E\{...\}$ denotes the expectation value.

In [7], Cloude and Pottier proposed a decomposition based on the projection of the polarimetric coherency matrix $[T]$ onto its eigenvalues basis. The matrix $[T]$ is given by a weighted sum of three unitary matrices of rank one, each representing a pure scattering mechanism $[T^{(i)}]$:

$$[T] = \sum_{i=1}^{3} \lambda_i [v]_i [v]^{*T}_i = \sum_{i=1}^{3} \lambda_i [T^{(i)}], \quad (9)$$

where $\lambda_1 > \lambda_2 > \lambda_3$ are the ordered eigenvalues and v_i its corresponding eigenvectors. The entropy H and anisotropy A have been defined as:

$$H = \sum_{i=1}^{3} -P_i log_3 P_i, \quad (10)$$

$$A = \frac{\lambda_2 - \lambda_3}{\lambda_2 + \lambda_3}, \quad (11)$$

where the pseudo-probabilities P_i are given by:

$$P_i = \frac{\lambda_i}{\sum_{j=1}^{3} \lambda_j}. \quad (12)$$

Also the α parameter is given as the weighted mean of the α_i parameters corresponding to the three scattering mechanisms [7]:

$$\alpha = \sum_{i=1}^{3} P_i \alpha_i. \quad (13)$$

The extracted two meaningful roll-invariant parameters H and α indicate the random behavior of the global scattering and, respectively, the mean scattering mechanism from surface to double bounce scattering. They are strongly related to the geophysical properties of the ground target area providing reliable classification information. In [7], nine clustering zones are proposed in the H and α plane.

Due to the strong influence of the polarization upon the estimate of the interferometric coherence, Cloude and Papathanassiou proposed a method for finding the optimal linear combination of polarization states [10]. The optimum scattering mechanism corresponds to the projection of both master and slave target vectors on the eigenvectors $[w]_{1_{opt}}$ and $[w]_{2_{opt}}$ of the maximum eigenvalues. The highest coherence γ_{opt1} is obtained by forming the interferogram between the two optimized scalar complex images μ_{1opt} and μ_{2opt}:

$$\mu_{1opt} \mu^*_{2opt} = [w]^{*t}_{1opt} [\Omega]_{12} [w]_{2opt}. \quad (14)$$

Based on the three optimized coherences $\{\gamma_{opt1}, \gamma_{opt2}, \gamma_{opt3}\}$, two characteristic indicators of the coherence distribution in the different optimized channels, A_1 and A_2, are introduced in [11, 12]:

$$A_1 = \frac{|\gamma_{opt1}| - |\gamma_{opt2}|}{|\gamma_{opt1}|}, A_2 = \frac{|\gamma_{opt1}| - |\gamma_{opt3}|}{|\gamma_{opt1}|}. \quad (15)$$

3. INTERACTIVE FUZZY FUSION SYSTEM

The second step of the proposed approach combines the information extracted from the SAR images. Expert knowledge is introduced by using an interactive symbolic fuzzy fusion (ISFF) method [13]. The interactive and symbolic aspects are the main keys of the method detailed hereafter.

3.1. Knowledge representation

The attributes to be fused are described by the experts by means of several symbols (words). These symbols are related to the attribute numerical values through the membership functions. For each attribute $A_i, i \in [1, N_A]$, where N_A is the number of attributes, a symbolic description is a set of s_i words denoted by:

$$\mathcal{L}_i = \{L_{i,1}, L_{i,2}, ..., L_{i,s_i}\}$$

The membership functions are set by the system with equidistant modal values, but they can be adjusted later by the user (Section 3.3).

The attributes represented by sets of symbols are aggregated according to the expert knowledge. This knowledge is modeled using the fuzzy subset theory, the experts being able to express their reasoning in a linguistic way by means of IF-THEN rules. A general rule example for the description of an output class is:

IF A_1 is $L_{1,j}$ AND A_2 is $L_{2,j'}$ AND ...
THEN pixel BELONGS TO out_k.

where $A_i, i \in [1, N_A]$ are the attributes, $L_{i,j}, j \in [1, s_i]$ the symbols that describe these attributes, and out_k is an output class, $k \in [1, N_C]$, where N_C is the number of classes.

The fuzzy subset theory is an adequate tool to encode such linguistic knowledge [14]. In this theory, a *rule-base* is used to represent all the rules. In a three-input fusion case, this rule-base can be described in the three-dimensional (3D) attribute domain where each sub-cube represents a rule for a desired output class.

3.2. Fusion principle/aggregation step

The numerical input attributes are processed according to the membership functions in order to obtain a linguistic description. The aggregation of the linguistic descriptions is then performed by Zadeh's compositional rule of inference [14, 15] in order to obtain at each pixel the membership degree μ_k to the output class k:

$$\mu_k(a_1, a_2, ...) = \bot_{L_{1j}, L_{2j'}, ... \in \mathcal{L}_1, \mathcal{L}_2, ...} \top\Big(\top(\mu_{D(a_1)}(L_{1j}), \mu_{D(a_2)}(L_{2j'}), ...), \mu_R(L_{1j}, L_{2j'}, ..., k)\Big) \quad (16)$$

where $(a_1, ...)$ are the values taken by the attributes $A_1, ...$ at the current pixel. The term $\mu_R(L_{1j}, ..., k)$ is equal to 1 if the corresponding rule is present in the *rule-base* and 0 otherwise. The fuzzy operators involved in this formula are chosen to obtain a system behavior close to the behavior of experts when they interpret images [13]. The selected operators are:

- $\top(a, b) = a * b$
- $\bot(a, b) = min(a + b, 1)$

Finally, the decision step consists in classifying the considered image pixels into output classes according to the greatest output membership degree μ_k.

3.3. Graphic user interface

The proposed approach involves experts in the fusion of the attributes. The experts' role consists in initializing the fusion system thanks to their experience. They give the rules which define the sought-after classes and they provide the membership functions in order to adjust the meanings of the words used in the rules. These parameters must be set in an interactive way, in order to allow them to improve the detection. The other steps of the fuzzy method (the inference rule and the combination/projection operator) are automatic: the end users are not expected to interact in these steps which require specific knowledge in the fuzzy subset theory.

A Graphic User Interface (GUI) has been developed to enable an interactive introduction of the expert knowledge into the fusion of three attributes. The GUI is composed of a 3D space where each axis corresponds to an attribute. The linguistic parameters and the rules are easily set by experts directly in the representation cube. For each rule, the corresponding sub–cube can be stretched and the membership functions which describe the symbols involved in the rule are automatically adjusted in the same 3D space. In order to help experts in this adjustment, different sets of points corresponding to reference regions (pointed out by experts or given by masks), can be drawn in the attribute space. The objective is then to stretch the sub–cubes in order to isolate the different sets of points as precisely as possible. Then the system is ready to perform the fusion. The fuzzy results can be observed as images of the membership degrees to the output classes. Crisp results are obtained either interactively by thresholding one of the membership degrees or automatically by selecting the output class which obtain the highest degree.

4. RESULTS AND DISCUSSION

The proposed method has been developed to deal with the high mountainous relief present in the Chamonix Mont-Blanc test site which is located in the Alps, near the borders between France, Italy and Switzerland ($45°50'$N, $6°51'$E). It includes the Aiguille-Verte (4122 m ASL), the Chamonix valley (1000 m ASL) and two instrumented glaciers: the Mer-de-Glace and the Argentière.

4.1. Multi-InSAR data

In this paper, 10 SAR images from ERS 1 and ERS 2 have been processed. This data set presented in Tab. 1 includes 1-day tandem couples in descending passes. After obtaining the SLC images, the five tandem interferograms were produced. Fig. 1 presents a color composition of three SAR amplitudes at three different months: July, December and April. One can notice that in Fig. 1, the grayscale regions correspond to non-changing features, while the colored regions exhibit an important change in radiometry.

After coarse radiometric corregistration of the five interferograms, the third order log-cumulant of the SAR amplitudes was computed within a $3 \times 3 \times 10$ neighborhood (Fig. 2-(a)). This parameter provides information on the stability of strong scatterers. The next processing step is to filter each interferogram independently using IDAN technique [6] by compensating the deterministic

Table 1. ERS SAR RAW data acquired over Mont-Blanc area with the frame number 2673 *and* B*: baselines (parallel and perpendicular to the radar line of sight).*

Dates	**Orbites**	$B_{\parallel}$ **(m)**	$B_{\perp}$ **(m)**
95.07.09/95.07.10	20823/01150	-4	29
95.10.22/95.10.23	22326/02653	-44	-107
95.12.31/96.01.01	23328/03655	79	208
96.03.10/96.03.11	24330/04657	26	9
96.04.14/96.04.15	24831/05158	39	93

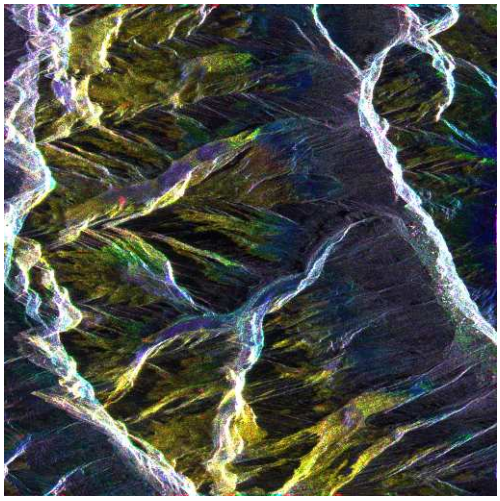

Figure 1. Chamonix-Mont Blanc [512×512 *pixels]: color composition of 10-looks SAR amplitudes (Red=1995/07/09, Green=1995/12/31, Blue=1996/04/14.)*

phase component [8]. Each interferogram provide an image which stores in each pixel the size of the neighborhood used in the interferogram estimation. The second attribute is obtained (Fig. 2-(b)) by taking the minimum over the five region size maps. Finally, the vector coherence (Fig. 2-(c)) is computed by employing Eq. 1 over a $3 \times 3 \times 5$ neighborhood.

Once the space defined by the three attributes from Fig. 2 is built, the 3D histogram is computed Fig. 3. As the third order log-cumulant provides information on the strong scatterers within the SAR amplitude images, its distribution presents a main lobe in the vicinity of $\tilde{\kappa}_3 = \mathbf{\Psi}''(10)$ and outliers corresponding to strong scatterers. This induces a non-uniform distribution of the words employed in the fuzzy fusion step. After visualizing the 3D histogram, the end-user must tune the partition of the attribute space, assuring enough word sampling in each cloud of points.

The final step, before starting the fusion is to assign the set of rules corresponding to the desired classes. This can be performed by:

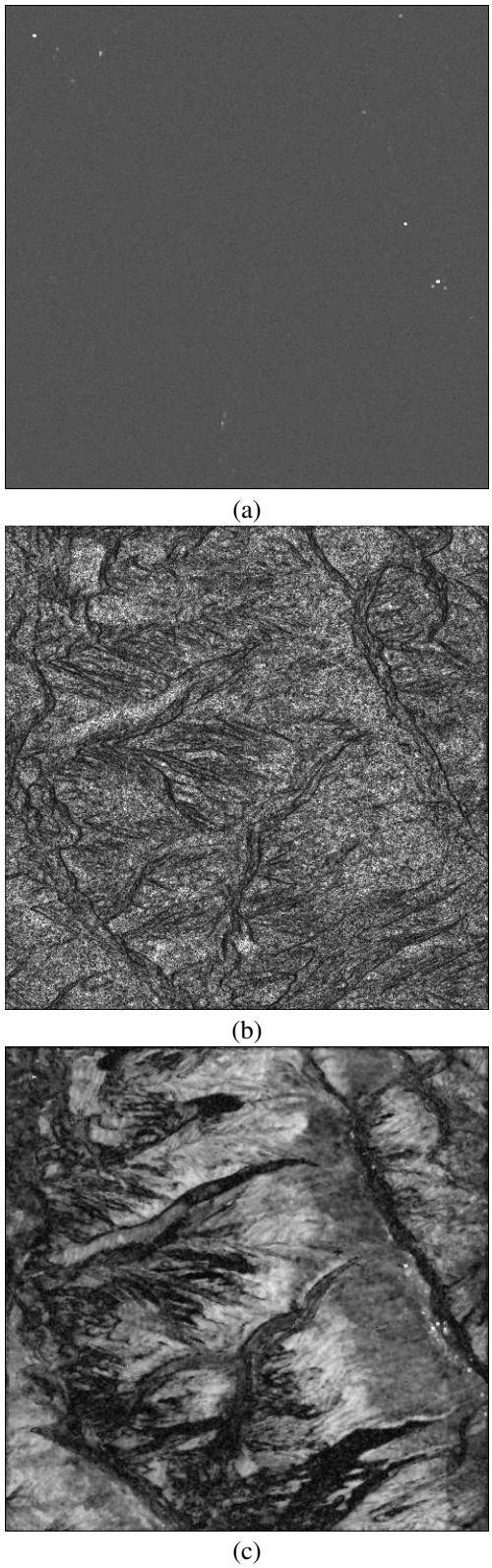

(a)

(b)

(c)

Figure 2. Multi-InSAR attributes [512×512 *pixels]: (a) third order log-cumulant, (b) region size, (c) vector coherence.*

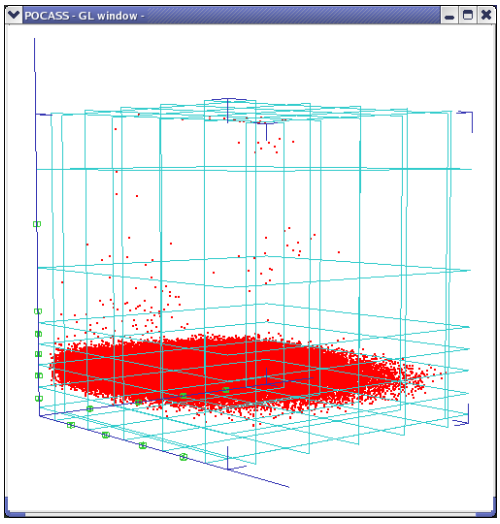

Figure 3. 3D histogram of the Multi-InSAR attributes from Fig. 2. The mesh within the attribute space corresponds to the interactive tuning of the words used in the fuzzy fusion (horizontal axes - vector coherence vs. region size; vertical axis - $\tilde{\kappa}_3$).

- expert (a priori) knowledge on the behavior of the attributes (ex: if the vector coherence and the third order log-cumulants are large and the regions size is small then the class is CSS);
- visualizing clouds of points corresponding to different region of interests which are candidates for the desired classes. This regions of interest can be selected on either one of the attributes or on another image easier to interpret (ex: one of the SAR amplitude images).

The detection result is presented in Fig. 4. The class marked in red represents the CSS points. As the obtained CSS points are only on non-moving areas (mainly in the Chamonix valley), CSSInSAR processing [5] for measuring glacier velocity is not applicable with ERS data on the studied glaciers. However an interesting result is observed on the upper area of the Argentière glacier (at the left of Fig. 4). This region has been detected as a stable distributed target area (marked in blue) and corresponds to the catchment area of the Argentière glacier (approximately over 2800m ASL). The green class represents the changing regions and is in accordance with mountainous vegetation areas next to the Chamonix valley, while the class represented in white is undecided.

4.2. POL-InSAR data

A new SAR airborne campaign took place in October 2006 over the two glaciers located in the Mont-Blanc area. Through a collaboration between the DLRs Microwaves and Radar Institute and the MEGATOR group (*http://www.gipsa.lis.inpg.fr/megator*), E–SAR repeat pass interferometric, polarimetric and multi-band

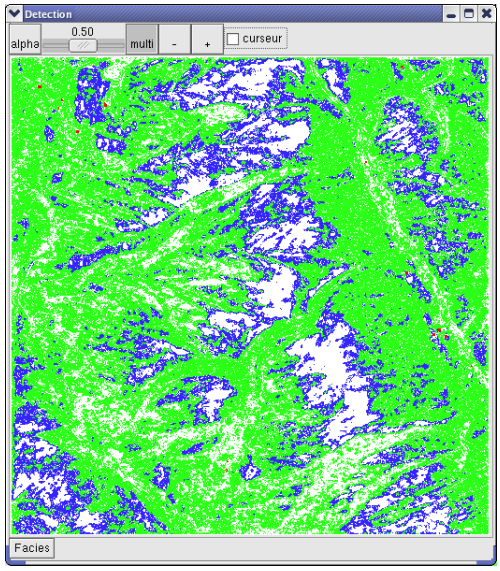

Figure 4. Multi-InSAR fuzzy fusion detection result: Red=CSS, Blue=stable distributed targets, Green=changing regions and White=undecided.

data have been acquired together with in situ measurements which provide useful information for the SAR synthesis, for the backscattered signal analysis and for performance assessment. In preparation for the processing of these future data, the present paper uses a well-known airborne data set, acquired in 1999 by the same E–SAR system. It represents a repeated pass, interferometric, fully polarimetric (monostatic mode) L-band (1.25 GHz) acquisition with a baseline of about 15 m. The spatial resolution is 1.5 m in range and azimuth. The target area Fig. 5 is the DLR headquarters (Oberpfaffenhofen area) from Wessling, Germany.

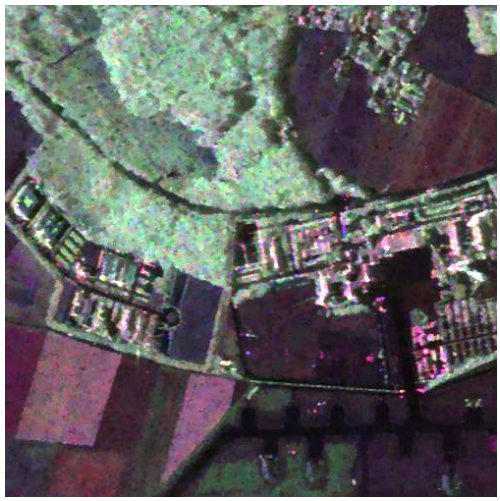

Figure 5. Oberpfaffenhofen [501×501 pixels]: color composition of IDAN estimated T_{11} diagonal terms.

In order to obtain a more robust estimation of the POL-InSAR coherency matrix, the IDAN estimation technique

was employed [6]. Then three attributes defining the 3D classification space are derived: entropy, mean alpha angle and A_2 (Fig. 6). These attributes provide useful information for separating different scattering mechanisms within the scene [7].

Fig. 7 presents the 3D histogram of the attributes from Fig. 6. As the distribution of points fills the entire 3D space, a fine uniform partition of the cube has been chosen (eight words on each of the three axes).

In order to assign the class rules, three regions of interest were selected on the POL-InSAR span image. These regions correspond to three different backscattering mechanisms: red for double bounce (buildings), blue for single bounce (fields) and green for volume scattering (forests). Then, the corresponding conditional histograms were plotted inside the attribute space. Finally, the rules were interactively assign such as they include these class prototypes. The fuzzy fusion classification result is presented in Fig. 8. Such a classification result may be used as input for automatic Wishart clustering of POL-InSAR data.

5. CONCLUSION

In this paper, a tunable fuzzy fusion system is proposed for the detection of specific features from multivariate SAR data sets, either multi-temporal InSAR or POL-InSAR. The nature of the application requires interaction between the intrinsic properties of SAR scatterers and qualitative information brought by experts. The proposed fusion system is designed to combine different sources of information by means of a fuzzy symbolic set of rules, the behavior of which is close to that of the end-user. The example presented on the Mont-Blanc temperate glaciers shows encouraging results in combining qualitative geophysical knowledge with objective parameters for detection-classification purposes: coherent and stable scatterers selection or change detection of distributed targets. In perspective, it will be interesting to use such approaches in the analysis of future POL-InSAR data acquired over Alpine glaciers.

ACKNOWLEDGMENTS

This work was supported by the French national project ACI-MEGATOR. The authors wish to thank to the European Space Agency for providing ERS SAR data through the Category 1 proposal No.3525. The authors wish to thank Dr. Irena Hajnsek (DLR - German Aerospace Center) for the POL-InSAR data set.

REFERENCES

[1] R. J. Braithwaite. Glacier mass balance: the first 50 years of international monitoring. *Prog. Phys. Geog.*, 26(1):76–95, 2002.

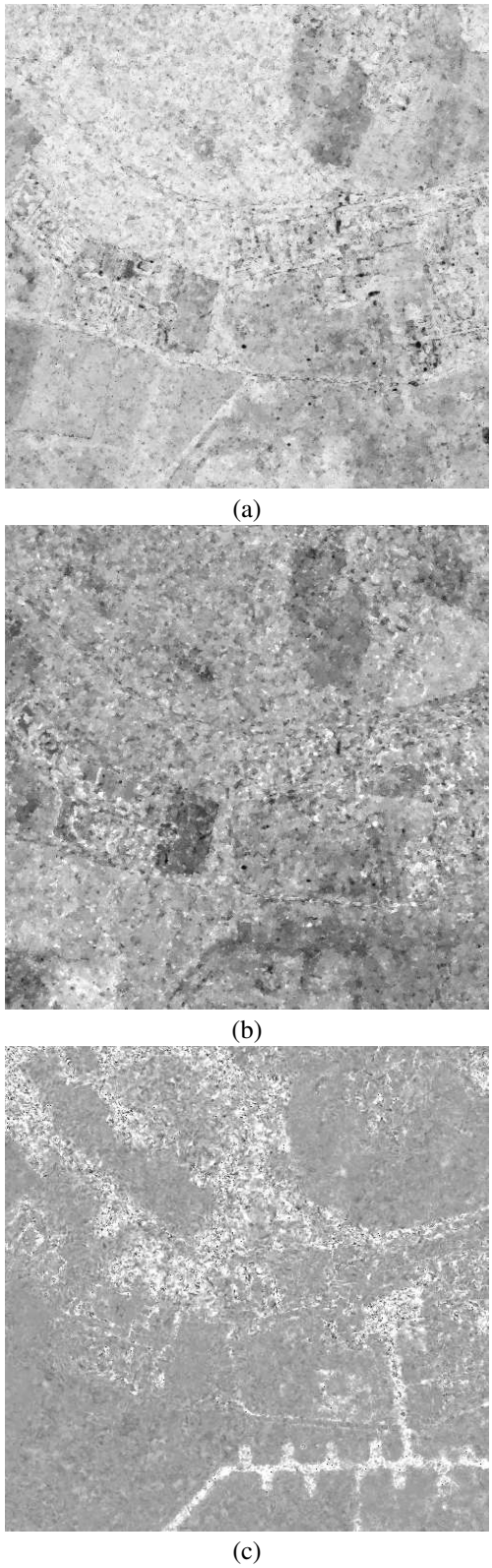

Figure 6. POL-InSAR attributes [501×501 *pixels]: (a) entropy, (b) mean alpha angle, (c)* A_2.

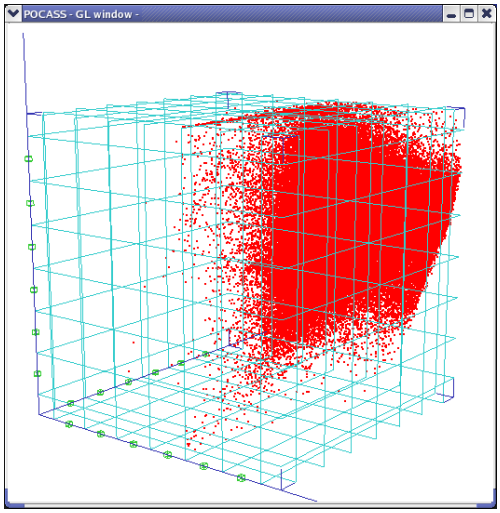

Figure 7. 3D histogram of the POL-InSAR attributes from Fig. 6. The mesh within the attribute space corresponds to the interactive tuning of the words used in the fuzzy fusion.

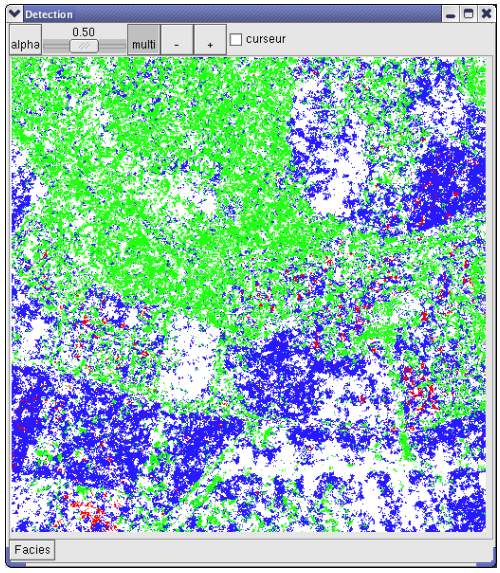

Figure 8. POL-InSAR fuzzy fusion detection result: Red=double bounce, Blue=single bounce, Green=volume scattering and White=undecided.

[2] D. Massonnet and T. Rabaute. Radar interferometry, limits and potential. *IEEE Transactions on Geoscience and Remote Sensing*, 31(2):455–464, 1993.

[3] E. Trouvé, G. Vasile, M. Gay, L. Bombrun, P. Grussenmeyer, T. Landes, J.M. Nicolas, P. Bolon, I. Petillot, A. Julea, L. Valet, J. Chanussot, and M. Koehl. Combining airborne photographs and spaceborne SAR data to monitor temperate glaciers. Potentials and limits. *IEEE Transactions on Geoscience and Remote Sensing*, (in print), 2007.

[4] J.C. Souyris, C. Henry, and F. Adragna. On the use of complex SAR image spectral analysis for target detection: Assessment of polarimetry. *IEEE Transactions on Geoscience and Remote Sensing*, 41(12):2725–2734, 2003.

[5] A. Hooper, H. Zebker, P. Segall, and B. Kampes. A new method for measuring deformation on volcanoes and other natural terrains using InSAR persistent scatterers. *Geophysical Research Letters*, 31(L23611):10.1029/2004GL021737, 2004.

[6] G. Vasile, E. Trouvé, J.-S. Lee, and V. Buzuloiu. Intensity-driven-adaptive-neighborhood technique for polarimetric and interferometric SAR parameters estimation. *IEEE Transactions on Geoscience and Remote Sensing*, 44(5):1609–1621, 2006.

[7] S.R. Cloude and E. Pottier. An entropy based classification scheme for land applications of polarimetric SAR. *IEEE Transactions on Geoscience and Remote Sensing*, 35(1):68–78, january 1997.

[8] G. Vasile, I. Petillot, A. Julea, E. Trouvé, Ph. Bolon, L. Bombrun, M. Gay, T. Landes, P. Grussenmeyer, and J.-M. Nicolas. High resolution SAR interferometry: estimation of local topography in the context of glacier monitoring. In *IEEE Geoscience and Remote Sensing Symposium Proceedings, IGARSS'06, Denver, USA*, (to appear) 2006.

[9] F. Bujor, E. Trouvé, L. Valet, J.M. Nicolas, and J.P. Rudant. Application of log-cumulants to the detection of spatiotemporal discontinuities in multitemporal SAR images. *IEEE Transactions on Geoscience and Remote Sensing*, 42(10):2073–2084, october 2004.

[10] S.R. Cloude and K.P. Papathanassiou. Polarimetric SAR interferometry. *IEEE Transactions on Geoscience and Remote Sensing*, 36(5):1551–1565, september 1998.

[11] L. Ferro-Famil, E. Pottier, and J.S. Lee. *Unsupervised classification of natural scene from polarimetric inteferometric SAR data*. C.H. Chen, Frontiers of Remote Sensing Information Processing edition, 2003.

[12] J.S. Lee, M.R. Grunes, T. Ainsworth, I. Hajnsek, T. Mette, and K.P. Papathanassiou. Forest classification based on L-band polarimetric and interferometric SAR data. In *POLinSAR 2005 Workshop CD-ROM, Franscati, Italy*, 2005.

[13] L. Valet, G. Mauris, P. Bolon, and N. Keskes. A fuzzy linguistic-based software tool for seismic image interpretation. *IEEE Transactions on Instrumentation and Measurement*, 52(3):675–680, 2003.

[14] L.A. Zadeh. Fuzzy sets. *Information and Control*, 8:338–353, 1965.

[15] D. Dubois, L. Foulloy, S. Galichet, and H. Prade. *Performing approximate reasoning with words - In Computing with words in Information/Intelligent systems 1*. Springer Verlag, 1999.